

**A Novel Hydroxyapatite-Containing 3-D Model
to Study the Effects of Mechanical Loading on
Breast Cancer Bone Metastasis**

Honors Thesis

Presented to the College of Arts and Sciences,

Cornell University

In Partial Fulfillment of the Requirements for the

Biological Sciences Honors Program

By

Min Joon Lee

May 2013

Supervisor: Claudia Fischbach-Teschl, PhD

Abstract

Breast cancer is the second leading cause of cancer-related deaths among women in the United States, and most of these deaths are due to metastasis to a secondary site, which is primarily the skeleton. The connection between primary breast cancer and frequent bone metastasis is poorly understood. Here, I investigate the role of two features of the bone microenvironment that may help elucidate this connection, the presence of mineral and mechanical stimuli. Bone marrow-derived mesenchymal stem cells (BM-MSCs) cultured with tumor-secreted soluble factors from bone-specific metastatic breast cancer cells deposited more mineral relative to factors from primary and lung-specific breast cancer cells, which could potentially explain the source of microcalcifications in the primary breast tumor. Additionally, I developed an *in vitro* loading system utilizing a mineralized 3-D model of the bone microenvironment. In the absence of loading, BM-MSCs in hydroxyapatite-containing (HA) scaffolds demonstrated enhanced osteoblastic activity compared to those in non-mineral-containing control scaffolds. Under compressive loading, BM-MSCs cultured with tumor-secreted soluble factors exhibited early commitment to the osteoblastic lineage. Loading did not affect breast cancer cell viability in this system, but expression of Runx2, a regulator of secretion of osteolytic proteins, was decreased 35% with loading. Taken together, these results suggest that bone marrow-derived stem cells are the source of microcalcifications, and metastatic tumor cells may affect the ‘vicious cycle’ by modulating the activity of osteoblasts and osteoclasts.

Keywords: breast cancer, metastasis, bone, loading, hydroxyapatite, microcalcification

Introduction

Breast cancer is the second leading cause of cancer-related deaths among women in the United States, and most of these deaths are due to metastasis to a secondary site, which is primarily the skeleton^{1,2}. Metastatic bone disease increases patient morbidity and mortality by promoting hypercalcaemia, spinal instability, pain, and bone fragility and fracture³⁻⁵. The link between primary breast cancer and its predilection for metastasizing to the skeleton is poorly understood. Here, I investigate the role of two unique facets of the bone microenvironment that may provide a favorable milieu for metastatic cells, the presence of mineral and mechanical stimuli. Firstly, microcalcifications in breast tissue share characteristics similar to mineral crystals in the skeleton, and they may be formed by stem cells recruited from the bone marrow⁶. Interactions between these microcalcifications and primary tumor cells may help drive metastasis to bone. Secondly, once these metastatic cells reach the skeleton, they exploit the bone remodeling process, but the effects of mechanical signaling in the metastatic niche may confer some protection against secondary tumor growth.

Breast microcalcifications, or the formation of calcified substrate within mammary tissue, have been linked to promotion of metastasis⁷. Clinically, they are used as a diagnostic marker for breast cancer⁸ and the degree of malignancy has been correlated with the specific type of microcalcification⁹. In particular, hydroxyapatite (HA), the prevalent inorganic mineral of the skeletal matrix, has been specifically associated with more malignant forms of breast cancer^{7,8}. Yet, the formation of microcalcifications, the molecular effects of microcalcification-breast cancer interactions, and their link in promoting bone metastasis remain poorly understood. Here, I hypothesized that bone marrow-derived mesenchymal stem cells (BM-MSCs) are the primary

source of breast microcalcifications and I examined the effects of tumor-secreted soluble factors on mineralization by BM-MSCs.

Mechanical stimuli in the skeleton plays a large role in regulating the process by which bone mass is maintained¹⁰. In healthy individuals, the homeostatic bone remodeling process includes degradation of the skeletal matrix by osteoclasts followed by new organic matrix being laid down by osteoblasts. However, in the presence of tumor cells, the relative activities of these two bone cells are dysregulated. In the ‘vicious cycle’ of bone metastasis, tumor-secreted soluble factors increase osteoclast-mediated osteolytic activity, which releases pro-tumorigenic factors from the skeletal matrix, ultimately favoring tumor settlement and growth¹¹. This cycle leads to bone loss and high risk for fracture. Increased mechanical loading results in net bone formation by increasing osteoblastic activity^{12,13} and physical activity is currently an approach for treating other forms of bone loss, such as osteoporosis¹⁴. Physical exercise could also potentially serve as an adjuvant therapy for bone metastasis patients^{15,16}. In fact, *in vivo* studies from our lab conducted by Dr. Maureen Lynch have shown that mechanical loading reduced secondary tumor growth and osteolytic degradation in tumor-bearing limbs through enhanced osteoblast activation and suppression of tumor-associated osteoclasts¹⁷, but whether or not loading directly affects tumor cells was not addressed by these previous studies. I hypothesized that mechanical loading would directly affect tumor cells, and have adapted a mineral-containing culture model so that I can apply mechanical loading in order to determine the role of loading in bone metastasis.

Materials and Methods

Characterization of BM-MSC Microcalcifications

To probe the genesis of breast microcalcification, I collected tumor-secreted soluble factors from primary, bone-metastatic, and lung-metastatic human breast cancer cells and observed their effects on bone marrow-derived mesenchymal stem cells (BM-MSCs) mineralization in two-dimensional (2-D) culture. To observe the effect of passage number on mineralization by BM-MSCs, the experiment was repeated using BM-MSCs at passage 4, 5, and 6. Mineralization was measured both qualitatively and quantitatively by Alizarin red staining, which stains for calcium deposition. Osteogenic differentiation was measured by alkaline phosphatase (ALP) activity. Positive and negative controls, those with osteogenic differentiation-inducing factors (+) or basal media only (-), were included.

Development of 3-D Mineralized Culture Model for BM-MSCs

To demonstrate the importance of mineral in creating a proper culture model of the bone microenvironment, Siddharth Pathi from our lab modified an established three-dimensional (3-D) *in vitro* scaffold system¹⁸ by incorporating HA, which tailors this system for modeling the bone microenvironment and secondary metastatic tumor growth^{19,20}. I cultured BM-MSCs in these HA-containing scaffolds for 60 days to demonstrate that BM-MSCs differentiation into bone cells and thrive in this model. Control scaffolds were prepared similarly without HA. Each scaffold type was randomized into osteogenically-induced or non-induced groups. Osteogenic differentiation was measured by ALP activity, collagen and mineral deposition via histological analysis, and gene expression of osteocalcin, a noncollagenous bone matrix protein. Mineralization was also assessed by utilizing micro-computed tomography and measuring compressive moduli.

Characterization of Loading Effects in a 3-D Culture Model

To investigate the direct effect of mechanical loading on metastatic breast cancer cell behavior, I applied mechanical loading to scaffolds seeded with primary breast cancer cells. For the effect of loading on cancer cells, I looked at genes commonly associated with bone metastasis (OPN, MMP1, and CXCR4)²¹ or osteolysis (IL-8, RANK, DKK, Runx2)²²⁻²⁷. In breast cancer cells, aberrant Runx2 activity is associated with metastasis and may also be related to paracrine signaling to bone cells²⁸. Additionally, to investigate if tumor-secreted factors interfered with the normal loading response of bone cells, I applied loading to BM-MSCs cultured in the presence of tumor cell-secreted factors. Expression of genes indicating osteoblast differentiation, Runx2²⁹ and osteocalcin³⁰⁻³², were quantified. Expression of SDF-1, a protein associated with recruitment of primary tumor cells to the skeleton and formation of the pre-metastatic niche³³, was also quantified.

Cell Lines and Culture

Bone marrow-derived stem cells (Lonza) were maintained in growth media (MSCGM, Lonza). Osteogenesis of BM-MSCs was induced by supplementing growth media with: 0.1mM dexamethasone, 50mM ascorbic acid-2-phosphate, and 1M β -glycerophosphate (Sigma). Cultures that had these supplements are hitherto referred to as 'induced' conditions; their corresponding controls 'non-induced.' Primary human metastatic breast cancer cells (MDA-MB231, 231, ATCC), and bone- (MDA-MB231-2287, 2287) and lung-specific (MDA-MB231-4175, 4175) subpopulations were maintained in complete Dulbecco's Modified Eagle Medium (cDMEM, DMEM [Invitrogen] supplemented with 10% fetal bovine serum [FBS, Tissue Culture Biologicals] and 1% penicillin/streptomycin [P/S, Invitrogen]). 2287 and 4175 are organ-specific

breast cancer sub-lines provided by Dr. Joan Massagué from Memorial Sloan-Kettering Cancer Center. All cell lines were cultured in 175cm² tissue culture flasks under standard cell culture conditions (37°C, 5% CO₂).

Preparation of Tumor-Conditioned Media

Tumor-conditioned media (TCM) from breast cancer sublines (231, 2287, 4175) were collected to study the effects of tumor-secreted factors on BM-MSC-driven microcalcification. Briefly, cancer cells were cultured in 175 cm² tissue culture flasks and maintained in cDMEM. 24 hours prior to collecting media, media was changed to low serum media (DMEM with 1% FBS and 1% P/S). TCM was concentrated ten-fold using Amicon Ultra-15 Centrifugal Filter Units (Millipore), and normalized by cell number. Control media was prepared with low serum media in the same manner. Concentrated TCM was then further diluted to two-fold in osteogenic media (231+, 2287+ 4175+) or in basal media (231-).

Fabrication of 3-D Hydroxyapatite-Containing (HA) Scaffolds

HA scaffolds were prepared from poly(lactide-co-glycolide) (PLG) and hydroxyapatite (HA) using previously established methods^{18,19}. Briefly, 8 mg of PLG microspheres (average diameter 5-50 µm), 8 mg of HA particles (Sigma, average diameter of 200 nm), and 152 mg of NaCl particles (J.T. Baker, size 250-425 µm) were cold pressed (Carver Press) into disks (1 mm thick, 8.5 mm diameter). These disks were subsequently subjected to a gas-foaming/particulate leaching technique that resulted in surface exposure of the incorporated mineral²⁰ (Fig. 1). PLG control scaffolds were prepared in the same manner without HA.

Scaffolds were sterilized with 70% ethanol, washed 4 times with sterile phosphate buffered saline, and seeded with 1.5 million cells per scaffold as previously described¹⁹. Cell-seeded scaffolds were pre-incubated on an orbital shaker at standard cell culture conditions for 3 days prior to differentiation or loading studies. Scaffolds were kept on the orbital shaker in between loading sessions. At the end of experiments, scaffolds were bifurcated and randomly assigned into groups for subsequent analysis (n=2-4/analysis).

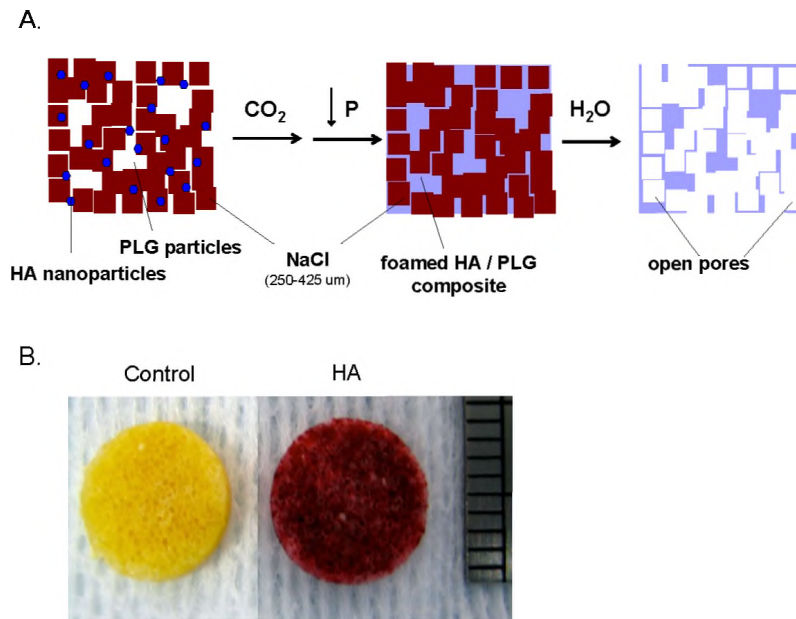


Fig. 1: Fabrication of HA scaffolds and PLG (control) scaffolds via a gas-foaming/particulate leaching technique. (A) After leaching out NaCl, open pores allow seeded cells to interact with 3-D matrices and form tissue. (B) Representative HA scaffolds stained for Alizarin red. HA scaffolds exhibit extensive surface exposure of incorporated HA both on the surface and inside the scaffolds (red), while control scaffolds do not (yellow). The resulting scaffolds are approximately 1 mm thick and 8.5 mm diameter.

BM-MSC Differentiation in 3-D Scaffolds

Alkaline phosphatase (ALP) activity (Thermo Scientific) was measured from cell lysates. ALP activity was normalized to either total protein (Bio-Rad Protein Assay, Bio-Rad) or DNA content (Quantifluor fluorescent dye, Promega). For histological analysis of protein deposition within the scaffolds, scaffolds were fixed for 1 hour, embedded in paraffin, and sectioned. Sections were stained with Masson's trichrome to detect collagen and mineral formation. All sections were stained in batch simultaneously to avoid variations in histology. Histological images were captured using an Aperio Scanscope (Aperio Technologies) and collagen content was quantified using ImageJ with RGB threshold for blue (RSB NIH). To measure overall mineral content, scaffolds were scanned using quantitative micro-computed tomography (microCT, Xradia) at 12.6 μ m isotropic voxel resolution. Each scaffold was manually segmented, and bone volume fraction (BV/TV) was quantified by dividing the mineral volume within the scaffold (BV) and the total volume (TV). Stiffness and Young's modulus were measured for HA scaffolds (Enduratec ELF 3200). Finally, scaffold contraction was measured.

3-D Mechanical Loading

Initially, cyclic hydrostatic pressure was applied to scaffolds via a hydraulic testing frame (MTS). Hydrostatic pressure was applied to cell-seeded scaffolds at 6MPa, 1Hz for 2 hours per day for 5 days in a custom-made pressure vessel set up³⁴. This approach did not result in changes for any of our conditions and was deemed inappropriate for differentiating BM-MSCs into osteoblasts instead of chondrocytes³⁴.

Therefore, I employed a mechanical loading system that applied compression directly to the scaffolds, inducing bone substrate deformation and fluid flow through the pores of the

scaffold, stimuli that bone cells typically experience in vivo³⁵. The loading platen of an established loading bioreactor was utilized for applying dynamic mechanical compression to scaffolds in a 24 well plate³⁶. In brief, after cell seeding, all scaffolds were randomized into loaded or non-loaded groups. Scaffolds then underwent dynamic loading for 3 days using parameters previously reported to stimulate osteoblasts (1Hz, 10% peak amplitude with a static offset of 5%, 1 hour per day)³⁷. Scaffolds were kept on an orbital shaker in between loading sessions. 24 hours after the final loading session, scaffolds were harvested for gene expression, DNA analysis, and live/dead staining. DNA was isolated using Caron's buffer and was quantified using a Quantifluor fluorescent dye. Live cells were stained with calcein and dead cells were stained with propidium iodide.

RNA Extraction and RT-PCR

Gene expression was analyzed using quantitative RT-PCR (qPCR) and the comparative ΔC_T method³⁸. Briefly, mRNA was isolated using the TRIzol extraction method³⁹ in RNase-free conditions. Quantitative PCR was performed using SYBR and primers of genes of interest and was normalized to the expression of β -actin (Supplementary Table 1).

Statistical Analysis

For the microcalcification study, the effect of TCM was compared between 2287 and other groups or 231 and other groups using one-way ANOVA. The effect of HA on ALP activity was compared between the experimental group and its corresponding control using one-way ANOVA. The effect of inducing factors was compared between the induced group and the non-induced group of each scaffold type separately using one-way ANOVA. The collagen content

was compared using a Student's t-Test. For the BM-MSCs differentiation study, experiments were performed in duplicate and results reflected pooled data. For *in vitro* loading, the effect of loading on gene expression was compared between the loaded and its corresponding non-loaded group using two-tailed t-tests. Experiments were carried out in duplicate and results reflected pooled data. Statistical significance (*) was set at $p \leq 0.05$. All values are represented as mean \pm SD.

Results

Tumor-Secreted Factors Increase BM-MSCs Differentiation in 2-D Culture

To observe to how breast cancer cells affect microcalcification formation by BM-MSC, the effect of tumor-secreted factors on BM-MSCs differentiation and mineralization was assessed. BM-MSCs were exposed to TCM from three different cancer cell sublines for two weeks. TCM with inducing factors collected from bone metastatic cells increased ALP activity the most relative to TCM from parental or lung metastatic cells (Fig. 2). No noticeable ALP activity was observed among cells cultured with basal media as well as cells cultured with 231 TCM without inducing factors (231-). Mineral content was consistent with corresponding ALP expression. Mineral deposition was greatest from BM-MSCs treated with bone metastatic breast cell-secreted factors, followed by parental breast cancer cells, both qualitatively and quantitatively assessed via alizarin red staining (Fig. 3). Overall, no mineralization was observed without osteogenic inducing factors with the exception of lung metastatic breast cancer cells, which had similar values as both positive and negative controls.

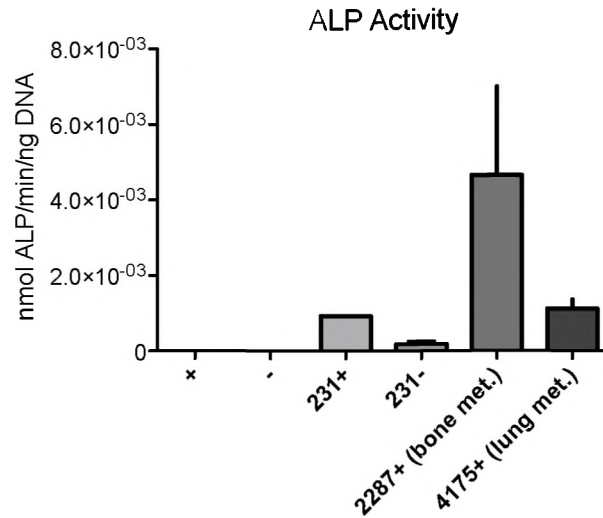
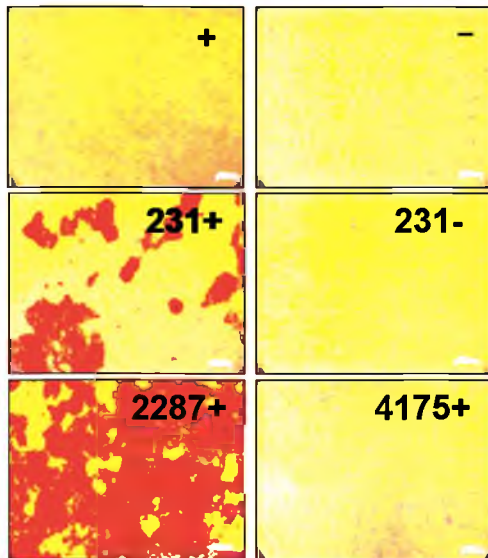


Fig. 2: Normalized ALP activity in lysates prepared from BM-MSCs cultured with tumor-conditioned media from breast cancer cell sublines, and with/without osteogenic inducing factors (+, -, respectively). Compared to the control+ and control-, BM-MSCs with soluble factors from bone-specific cancer cells (2287+) had the highest levels of ALP activity. Those from parental (231+, 231-) and lung-specific cancer cells (4175+) had less ALP activity than those from 2287+.

A.



B.

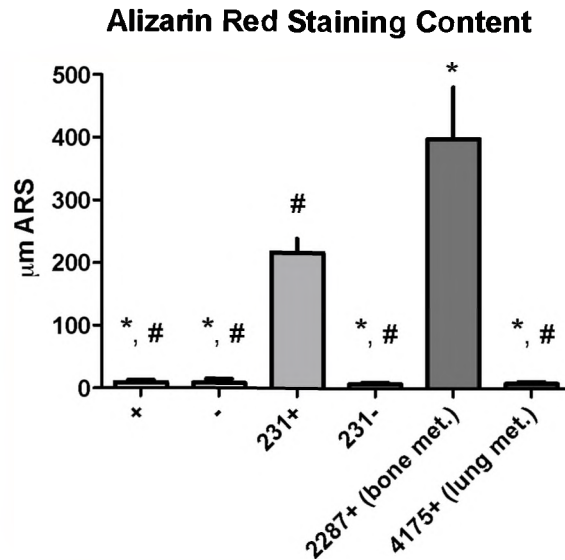


Fig. 3: Mineralization in response to tumor-conditioned media. (A) Representative images of alizarin red staining for all tumor conditions and with/without osteogenic inducing factors (+, -, respectively). BM-MSCs cultured with both TCM and osteogenic factors deposited visible mineral, with the exception of the lung metastatic group (4175+). Scale = 500 μm (B) Quantification of alizarin red staining via stain extraction. Only bone-specific (2287+) and parental cancer cells (231+) showed significantly greater mineral content compared to the controls. *main effect of soluble factors from MB231+ (vs. other groups). # main effect of soluble factors from 2287+ (vs. other groups).

These results were consistent with previous studies done by a co-worker in our lab, but ALP activity and mineral were significantly lower, especially from the positive control group. Because the current studies were conducted with BM-MSCs at passage 6, while previous studies were with those at passage 4, I examined whether differentiation and mineralization was

passage-dependent. ALP activity decreased from passage 4 to 5, and then increased from passage 5 to 6 (Fig. 4). However, the pattern of relative ALP activity among the sublines was consistent within each passage and with the previous study, with the exception of ALP expression from lung metastatic cancer at passage 6, which expressed relatively low activity across all passages. Similar to ALP activity, mineral content as measured by Alizarin red staining decreased from passage 4 to 5, but increased at passage 6. On average, BM-MSCs cultured with parental and bone metastatic factors mineralized more than those with lung.

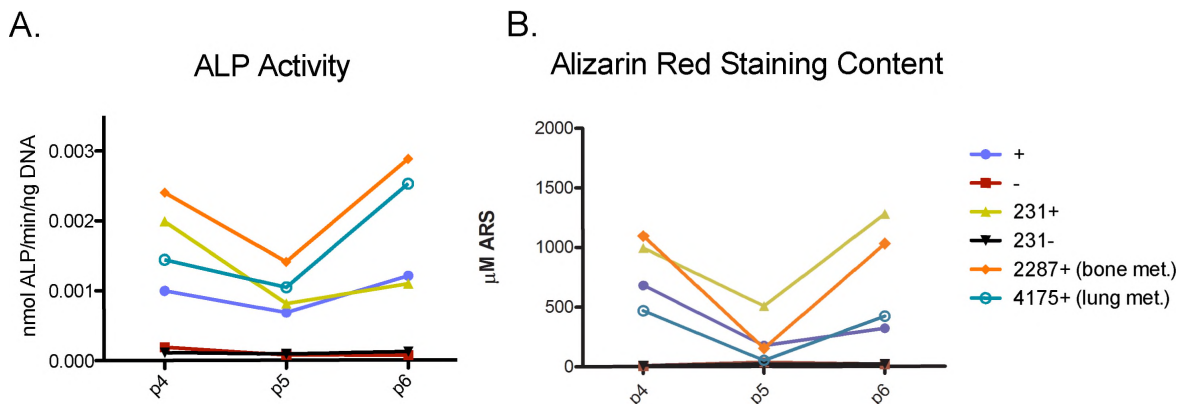


Fig. 4: Passage dependency of BM-MSCs differentiation and mineralization. (A) Normalized ALP activity decreased from passage 4 to 5, then increased at passage 6. The pattern – 2287+ having the greatest, following by controls – was consistent among all the passages, except for lung metastatic at passage 6, which expressed relatively low activity across all passages. (B) Mineral content decreased from passage 4 to 5, then increased at passage 6. Relative values within each passage were consistent.

HA-Containing Scaffolds Promote BM-MSCs Differentiation into Osteoblasts

Cells in 3-D culture form more natural cell-cell interactions and closely mimic tissues *in vivo*, so Siddharth Pathi from the Fischbach lab developed a 3-D culture model of the bone microenvironment. To study how effectively our scaffold system promotes the differentiation of BM-MSCs into mature osteoblasts, I seeded BM-MSCs into HA scaffolds or non-mineral-containing PLG scaffolds (control) and cultured them for 60 days. As expected, BM-MSCs cultured with osteogenic factors showed significantly elevated markers of osteoblast differentiation relative to control scaffolds. Non-induced cells in PLG scaffolds showed no ALP activity, while non-induced cells in HA scaffolds showed measurable ALP activity (Fig. 5). This result was further supported by collagen deposition. Induced cells in HA scaffolds showed the most collagen deposition both on the surface of and within scaffolds relative to all other groups (Fig. 6A, B). Similarly, gene expression for osteocalcin was also elevated for cells in induced HA scaffolds compared to control scaffolds.

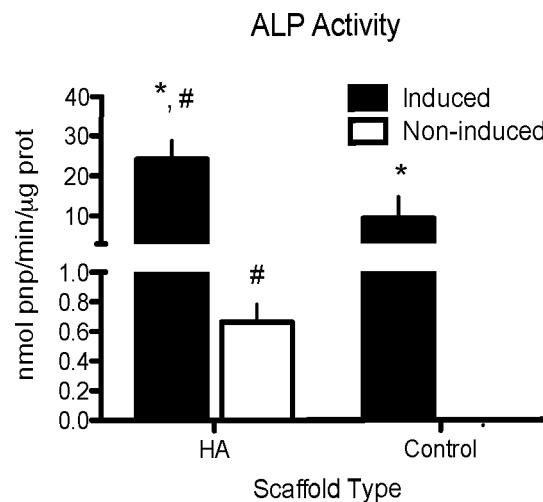


Fig. 5: Normalized ALP activity in lysates prepared from BM-MSCs in HA and PLG (control) scaffolds via colorimetric assay analysis. Osteogenic inducing factors promoted significantly

more ALP activity for BM-MSCs in both HA and control scaffolds, and the presence of HA in scaffolds further enhanced this response. #main effect of HA on ALP activity of BM-MSCs (vs. corresponding control scaffold), *main effect of osteogenic inducing factors on ALP activity of BM-MSCs (vs. corresponding non-induced group).

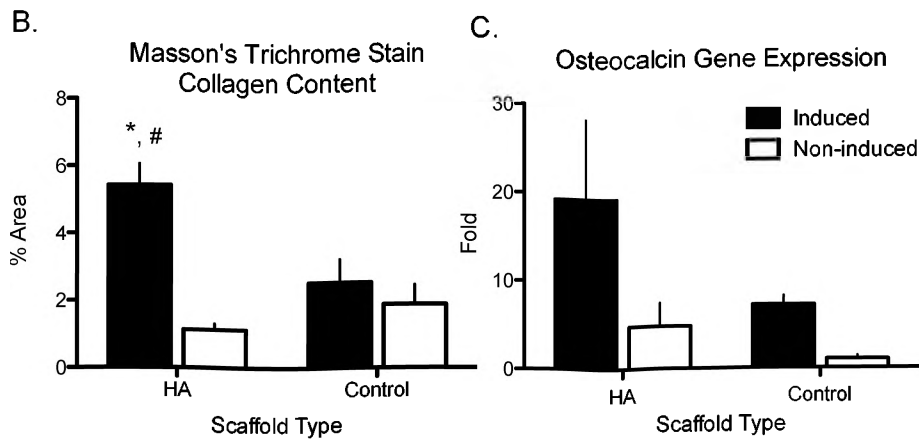
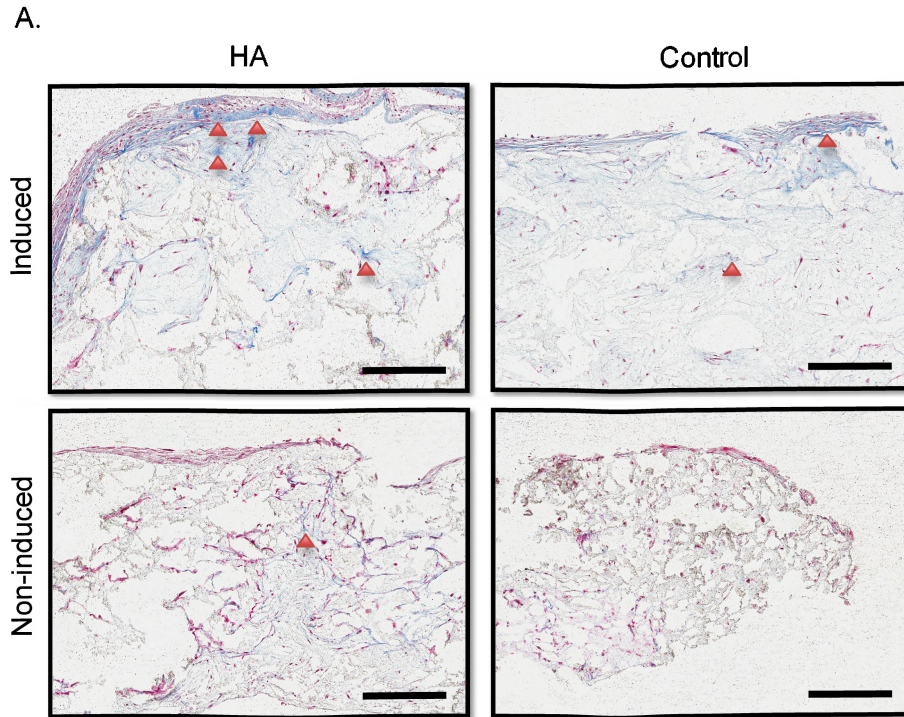


Fig. 6: Protein deposition and osteocalcin gene expression following 60 days of osteogenic culture. (A) Representative image of scaffolds after Masson's trichrome staining. BM-MSCs in induced HA scaffolds had the most collagen deposition (blue, represented by arrows) both on the surface and inside the scaffolds. Scale = 200 μm (B) % Area covered by collagen (blue) was 2-fold greater in induced HA scaffolds than in induced control scaffolds while collagen content did not change with induction in control scaffolds. (C) Osteocalcin gene expression was the greatest for cells in induced HA scaffolds. *HA induced vs. Control induced, # HA induced vs. HA non-induced.

To further quantify the amount of new bone formation by BM-MSCs in HA scaffolds, I measured total mineral content via microCT analysis. Induced HA scaffolds had greater BV/TV (160%) than those without osteogenic factors (Fig. 7B). Similarly, a trend was noted for greater compressive stiffness of HA scaffolds with osteogenic factors (Fig. 7C). The scaffolds with osteogenic factors deposited more minerals on the surface as well as inside than those without (Fig. 7A). Furthermore, both induced and non-induced HA scaffolds maintained their shape throughout 60 days, while both PLG types substantially contracted (Supplementary Fig. 1). Taken together, these results suggest that HA scaffolds not only provide a viable 3-D environment to the cells tested, but also a functional milieu in understanding cell-mineral interactions in the context of breast cancer bone metastasis¹⁹.

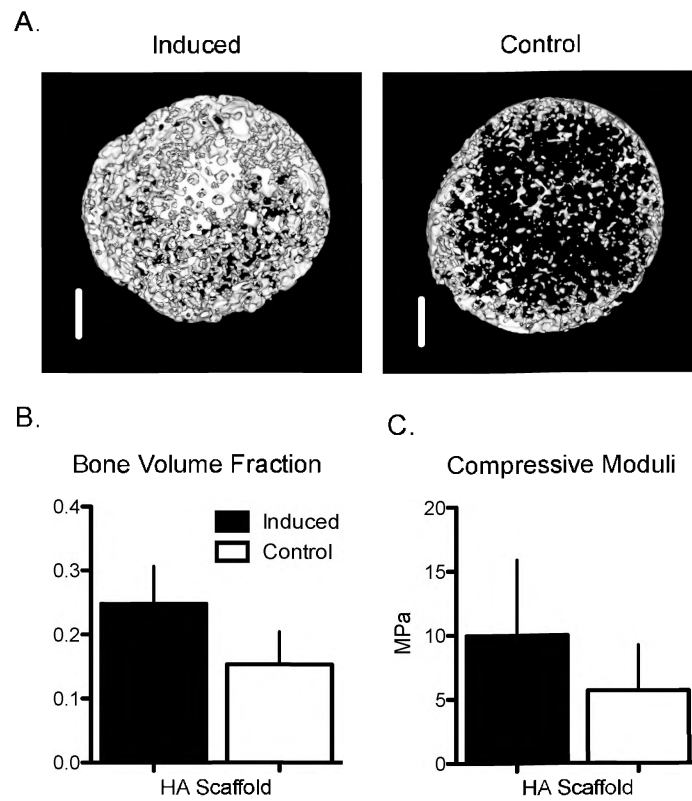


Fig. 7: Influence of osteogenic factors on BM-MSc mineralization and stiffness. (A) Representative images of induced and non-induced (control) HA scaffolds taken following 60-day culture period. 3-D microCT images demonstrate that osteogenic factors resulted in greater mineral content. Bar = 1mm. (B) Bone volume fraction increased (160%) in the presence of osteogenic factors compared to the control (N=2 per condition). (C) Increased mineralization resulted in a trend for greater stiffness (N=3 per condition).

In Vitro Tumor Cell Response to Mechanical Loading

Dr. Lynch has previously shown that mechanical loading of mouse tibiae *in vivo* reduced cancer-mediated osteolysis¹⁷. To delineate the underlying mechanism of the loading-mediated bone homeostasis, I first studied the direct effect of loading on MDA-MB231 (MDAs) in HA

scaffolds. Prior to cell studies, Praveen Polamraju from the Fischbach lab determined the mechanical characteristics of the scaffolds to ensure that the mechanical loads that I applied were within the elastic range. To this end, Praveen measured the compressive Young's modulus and yield strain of acellular HA scaffolds under quasi-static uniaxial compression, which were determined to be 290 ± 20 kPa and $29 \pm 9\%$ strain, respectively (Fig. 8A), indicating that 10% peak applied strain is well within the elastic range of the scaffolds. He also confirmed that our dynamic loading did not induce plastic strain hardening over time (data not shown). Following 3 days of mechanical loading, MDA viability and proliferation were similar between loaded and nonloaded groups (Fig. 8C-D). Next, I examined the effect of mechanical loading on changes in expression of genes associated with metastasis. Interestingly, loading did not alter expression of bone metastasis-specific genes (OPN, MMP1, CXCR4)²¹ or genes associated with osteolysis (IL-8, RANK, DKK)²²⁻²⁷ (Table 1). However, expression of Runx2 was reduced 35% with loading (Fig. 8E). Runx2 is a transcription factor that is aberrantly expressed by tumor cells and is associated with their ability to cause osteolysis^{26,27}. Runx2 also modulates production of proteins secreted by tumor cells, such PTHrP, that affect bone cell remodeling. Taken together, these results suggest that tumor cells are not directly affected by loading, but loading instead may modulate downstream effects on osteoblasts and osteoclasts.

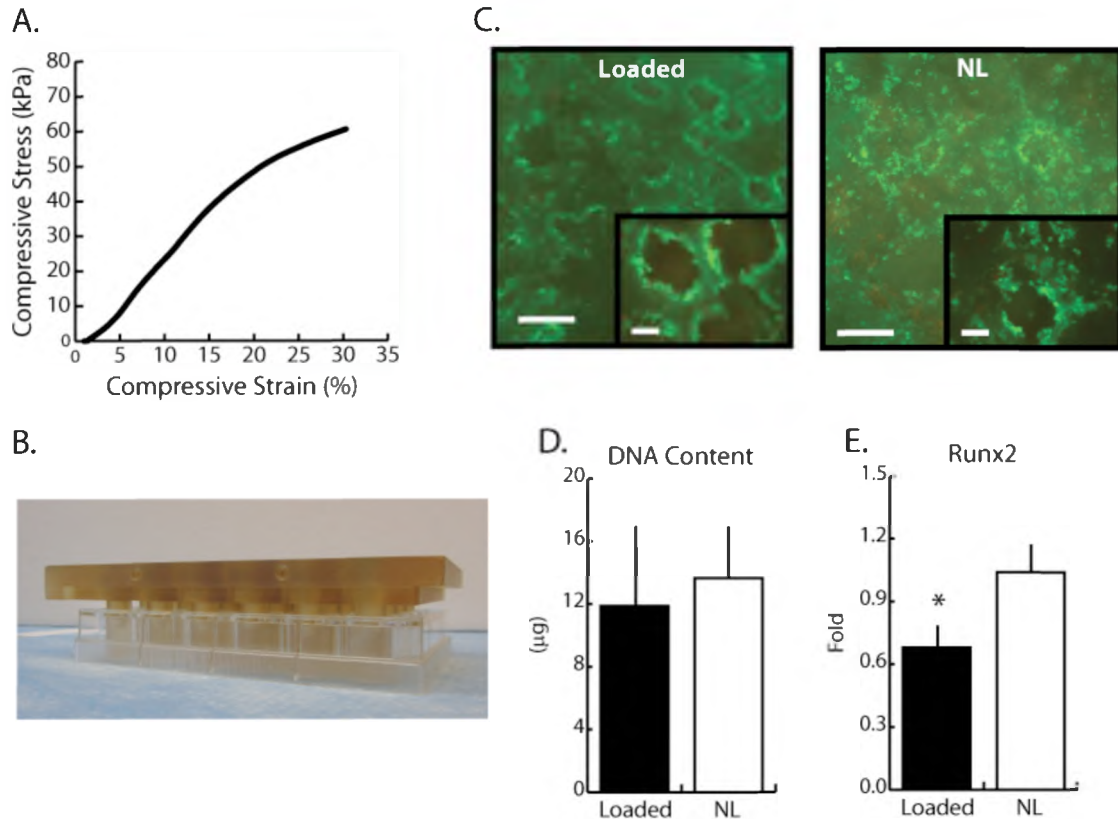


Fig. 8: (A) Representative stress vs. strain curve for HA scaffolds undergoing quasi-static mechanical compression. Young's modulus and compressive strain of the scaffolds were 290 ± 20 kPa and $29 \pm 9\%$ strain, respectively, ensuring that loading was performed in the linear elastic region of the HA scaffolds. (B) Loading platen used for loading MDA-MB231 tumor cell-seeded scaffolds in a 24 well plate for use in an established loading bioreactor³⁶ (C) Representative image of live and dead staining with calcein (green) and propidium iodide (red). Viability of MDAs within scaffolds was not adversely affected by compressive loading. Bar = 500 μ m (inset = 100 μ m). (D) Total DNA content per scaffold as measured via fluorimetric analysis and (E) relative gene expression of Runx2 as determined via qPCR following 3 days of loading. DNA content was similar between MDAs in both loaded and nonloaded (NL) scaffolds, while Runx2 expression was reduced 35% in loaded cultures.

Table 1: Primers used for qPCR and their expression in loaded groups relative to nonloaded groups. Other than Runx2 expression, changes in other gene expression of loaded groups were not significant compared to their respective non-loaded groups.

Gene	Name	Fold expression normalized to NL
<i>Runx2</i>	runt related transcription factor 2	0.68 \pm 0.1
<i>RANK</i>	Receptor Activator of Nuclear Factor κ B	0.87 \pm 0.1
<i>DKK1</i>	dickkopf 1 homolog	1.15 \pm 0.2
<i>OPN</i>	Osteopontin	1.20 \pm 0.6
<i>IL-8</i>	interleukin 8	1.06 \pm 1.0
<i>MMP1</i>	matrix metalloproteinase 1	0.85 \pm 0.1
<i>CXCR4</i>	chemokine (C-X-C motif) receptor 4	1.32 \pm 0.6
<i>Actb</i>	beta-actin	reference gene

Tumor-Associated BM-MSCs Response to Mechanical Loading

To observe the effect of metastatic cancer cell secretions on the loading-response of BM-MSCs, I applied mechanical stimuli for 3 days in the presence of tumor-soluble factors (TCM). Similar to MDAs, BM-MSCs proliferation was not affected by mechanical loading (Fig. 9A) or by the presence of tumor-secreted factors (data not shown). I also examined the effect of mechanical loading and TCM on changes in gene expression in BM-MSCs. With loading, the expression of Runx2 was increased by 42% compared to those of control (Fig. 9B). The expression of SDF-1 and osteocalcin was not significantly different between loaded and nonloaded groups. Taken together, these results suggest that BM-MSCs have increased osteoblastic activity with loading in the presence of tumor-secreted factors.

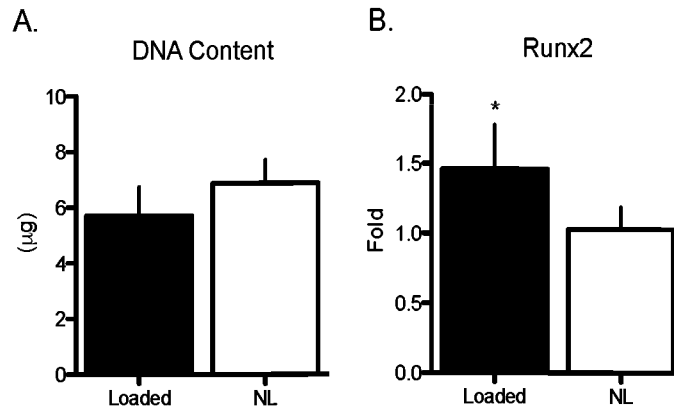


Fig. 9: Effect of loading on BM-MSCs cultured with TCM. (A) Total DNA content per scaffold as measured via fluorimetric analysis and (E) relative gene expression of Runx2 as determined via qPCR following 3 days of loading. DNA content was similar between BM-MSCs in both loaded and nonloaded (NL) scaffolds, while Runx2 expression was increased 42% in loaded cultures. * Main effect of loading (vs. NL group).

Discussion

In this study, I examined breast cancer bone metastasis in two different microenvironmental settings: first, primary breast cancer cell-microcalcification interactions in the breast microenvironment; second, metastatic breast cancer cell-loading interactions in the bone microenvironment. I showed that bone-marrow derived stem cells (BM-MSCs) are capable of forming microcalcifications under the influence of breast cancer cell secretions. I also showed that mechanical loading reduced the expression of Runx2, a modulator of breast cancer bone metastasis. These results will help uncover the underlying mechanisms for breast cancer so frequently metastasizing to the skeleton.

When BM-MSCs were cultured with tumor cell-secreted factors, differentiation and mineralization was greater with factors from bone-specific breast cancer cells than with those

from parental or lung-specific breast cancer cells, and this was independent of stem cell passage number. One plausible explanation is that while tumors secrete factors that increase osteolytic activity, they may also upregulate osteoblastic activity²⁴. With breast cancer that has metastasized to the skeleton, however, on balance, they disrupt the bone remodeling process by activating osteoclastic more than osteoblastic activity. Tumor-secreted factors may require osteoblastic differentiation as an indirect way to stimulate osteoclast formation²⁴. Co-culturing pre-osteoblasts and pre-osteoclasts with tumor-secreted factors would directly address this question.

My data suggest that bone metastatic breast cancer cells secrete factors that influence bone marrow progenitor differentiation into a mineral-producing cell phenotype, and this may be the mechanism underlying microcalcification formation in the breast. While this study was not sufficient to show the mechanisms of forming microcalcification, it suggests the importance of tumor-secreted factors in facilitating mineral formation. Although extensive studies must be done before therapeutic targets are identified, further characterization of the cross-talk between breast cancer and stromal cells will help explain the high rate of metastasis to the skeleton.

Studies conducted by scientists in the Fischbach lab have shown that bone marrow progenitors are recruited to the primary tumor site, which in turn enhances breast cancer metastasis to bone (Fischbach lab manuscript in preparation). The studies presented here suggest that the recruited bone marrow progenitors deposit minerals upon paracrine interactions with native cancer cells. This, in turn, provides a positive feedback loop that, based on our *in vitro* studies of BM-MSCs embedded in mineralized scaffolds, further enhances bone formation that could be the microcalcifications that seen in breast cancer patients. Investigating the effects of loading on mineral deposition of BM-MSCs in a 3-D tumor model¹⁸ may reveal another

mechanism by which primary breast cancer cells are transformed into bone-homing metastatic cells.

When I compared relative differentiation of BM-MSCs based on passage number, I did not see a clear pattern. I expected to observe decreased differentiation and mineralization of BM-MSCs with later passages because murine bone marrow-derived mesenchymal stem cells had been shown to exhibit decreasing osteogenic capacity with later passages (p6 vs. p1)⁴⁰. Here, I compared three consecutive passage numbers (p4-p6), and it is possible that the relative differentiation capacity of BM-MSCs at these later passages is not as significantly different as when comparing p1 to p6. Nonetheless, it would be more beneficial and physiologically relevant to use even lower passage number cells to observe clinically relevant cancer-stromal stem cell interactions⁴¹.

My static cultures of BM-MSCs and MDA-MB231 in HA scaffolds suggest an important role of HA in cell behavior. BM-MSCs in HA scaffolds showed significantly higher ALP activity than those in control scaffolds independent of inducing factors, suggesting that HA alone stimulates osteogenic differentiation of BM-MSCs. As expected, this effect was further elevated with inducing factors, which increased ALP, collagen and mineral deposition, and osteocalcin expression by BM-MSCs. Cell characteristics from the 3-D BM-MSCs differentiation study are consistent with *in vivo* osteoblastic behavior and clearly support my hypothesis that our 3-D mineralized model is appropriate for recapitulating the bone microenvironment. As for the response of tumor to the mineralized environment, MDA-MB231 in HA scaffolds increased expression of soluble factors related to the formation of osteolytic lesions (IL-8)⁴² and bone-metastatic capability (OPN, MMP1, CXCR4)²¹ compared to PLG scaffolds, indicating that mineral could have a role in facilitating breast cancer bone metastasis also (data not shown).

Over my 60-day differentiation study, the HA scaffolds maintained their architecture both in the presence and absence of osteogenic factors. HA scaffolds shrank the least, followed by PLG control scaffolds, which were markedly contracted. Since all acellular scaffold types maintained their original shape, scaffold contraction was not due to media-related degradation. Instead, osteoblasts likely pull on the scaffold matrix and remodel it via enzymatic reactions, resulting in contraction. Also, the mineral provides additional mechanical strength, helping scaffolds to retain their shape better during the scaffold-cell interaction⁴³. Since PLG scaffolds do not contain mineral, however, they could be degrading faster during cell interactions.

To probe the effect of loading on BM-MSCs and MDA-MB231 behavior, I initially employed two different loading systems: hydrostatic loading and compressive loading. Hydrostatic loading alone did not increase ALP or total protein expression of BM-MSCs (Supplementary Fig. 2), thus I next chose a loading system that applies compressive loading to the entire scaffold. This type of loading results in both fluid flow shear stress throughout the scaffold's pores and substrate deformation. Physiologically, the skeleton experiences various loading modalities simultaneously, but the effects of hydrostatic pressure on bone cells is probably negligible relatively to fluid flow and matrix deformation, which typically elicit very robust responses³⁵.

My results from *in vitro* mechanical loading of breast cancer cells suggest that while loading itself does not alter tumor cell viability or growth, it may have an effect on expression of genes that modulate homeostatic bone remodeling. Bone metastatic breast cancer cells exhibit a 'bone metastatic signature' that includes increased expression of (OPN, MMP1, and CXCR4)²¹. They also highly express genes related osteolytic remodeling (IL-8, RANK, DKK, Runx2)²²⁻²⁷. My mechanical loading studies showed no changes in gene expression of the bone metastasis

signature or of osteolysis, except for reduced Runx2 levels. Runx2 stimulates osteolysis by upregulating PTHrP-induced RANK secretion by osteoblasts, which in turn, activates osteoclast activity⁴⁴, and its abolishment minimized osteolysis²⁵. Furthermore, Runx2 also decreased osteoblast differentiation by modulating secretion of sclerostin, an inhibitor of Wnt signaling (i.e., a major regulatory pathway of skeletal biology)^{27,28}. Both our *in vivo* and *in vitro* studies suggest that mechanical loading may reduce osteolysis by promoting osteoblastic over osteoclastic activity. Further studies are needed to understand how loading-mediated reduction in Runx2 expression alters cell signaling pathways that ultimately may reduce breast cancer bone metastasis.

Similarly, mechanical loading of BM-MSCs, even in the presence of tumor-secreted factors, did not affect cell viability or growth. Early commitment of BM-MSCs to the osteoblastic lineage was greatest with loading in the presence of TCM, as determined by expression of Runx2, here an indicator of differentiation^{30,31}. Three days of loading was likely insufficient to see the changes in osteocalcin expression since it is a marker for late-stage osteoblast differentiation³². Taken together, results from our *in vitro* loading studies suggest that secreted factors from MDAs are driving the effects of loading in preventing secondary tumor growth and osteolysis *in vivo*¹⁷. A limitation of the current BM-MSCs loading study is that tumor-conditioned media was not collected from loaded MDAs. Future work should include loaded TCM to fully characterize the effects of loading on tumor cell-secreted factors and their role in subsequent bone cell behavior.

Mechanical stimulation is often recommended for patients with pathological bone loss (e.g., osteoporosis) to maintain or increase the bone mass¹⁴. This could be similarly used for patients who have metastatic bone disease. Clinically, physical therapy has shown to improve

patients' prognosis and quality of life undergoing or recovering from chemotherapy^{15,45,46}. However, the specific role of physical stimulation in preventing or treating bone metastatic disease or other secondary tumor growth has been unknown. Results from loading breast cancer both *in vivo*¹⁷ and *in vitro* collectively suggest that mechanical loading inhibits pro-osteolytic behavior of bone metastatic breast cancer cells. Although further investigation is necessary to understand how mechanical stimulation will be translated to the clinic, our results propose a potential starting point to consider incorporating physical therapy into treating or preventing cancer-associated osteolysis. Physicians often discourage prescribing high-impact exercise – the most effective way of improving bone density^{47,48} – to patients with advanced bone metastatic disease, as they are more susceptible to skeletal fragility and pain³⁻⁵. Therefore, physical therapy may be more effective in earlier stages of breast cancer.

My results present a functional link between mechanical loading and breast cancer-associated osteolysis, and suggest many interesting future studies. For example, determining whether loaded cancer cells in bone become dormant, undergo apoptosis, or metastasize to different organs is important for fully understanding the role of loading in metastasis. Using this 3-D loading model employed here, investigating dormancy and apoptosis could be tested by loading MDAs for a longer period of time (e.g., 4 to 6 weeks as done for our *in vivo* study¹⁷). Additionally, an altered phenotype under loading may suggest metastasis to other organs. For example, expression of genes commonly associated with metastasis to other sites (e.g. lungs, liver, brain)⁴⁹ could be examined (e.g., lung colonization with high expressions of CD44v⁵⁰, COX2, EREG⁵¹). Furthermore, it remains unknown whether different magnitudes of compression or other loading modalities affect tumor cell behavior. These aspects of mechanical loading need to be investigated in order to better understand the underlying mechanisms of

physical stimuli on primary as well as metastatic tumor sites, and to develop feasible therapy for patients prone to skeletal fracture and pain.

Conclusions

Microcalcifications in the primary tumor likely arise from interactions between breast cancer and BM-MSCs in the breast microenvironment. Additionally, mechanical loading inhibits tumor-associated osteolysis in the bone microenvironment by modulating osteoblastic and osteoclastic activities in bone remodeling homeostasis rather than by directly affecting tumor cell viability. To demonstrate this, I adapted a HA-containing scaffold to create a physiologically relevant culture model to study cancer metastasis in bone to which we could apply mechanical loading. Further studies are necessary to understand a functional link between the genesis of microcalcification and bone metastasis and to fully understand underlying molecular mechanisms of what has been seen *in vivo*. Similarly, studying mechanical loading to suppress tumor-associated bone diseases will help explore mechanical stimuli as an important microenvironmental parameter for treating bone disease patients.

Acknowledgements

The author gratefully acknowledges Dr. Claudia Fischbach-Teschl and Dr. Maureen Lynch for guiding him throughout his undergraduate research career. He would also like to thank Young Hye Song for helping with the microcalcification study, Praveen Polamraju for analyzing the HA scaffold mechanical properties, and the rest of the Fischbach lab members for providing feedback on his projects. Funding sources: NIH/MRRCC 5P30 AR046121-09, 1R01CA173083,

R21CA157383, a Summer Undergraduate Research Fellowship by the NYSTEM, and an Individual Biomedical Research Award by the Hartwell Foundation.

Accomplishments

The author is a recipient of the prestigious Summer Undergraduate Research Fellowship awarded by the New York State Stem Cell Science (NYSTEM), which led him to a poster/oral presentation at Summer Institute for Life Sciences (SILS) Undergraduate Research Symposium and BioExpo at Cornell University. His work also led him to an oral presentation at the national Biomedical Engineering Society (BMES) Annual Meeting at Atlanta, GA in 2012. Finally, his contribution to the project was honored with a co-authorship on a manuscript submitted to the *Journal of Bone and Mineral Research*.

Presentations:

Lee, M.J.; Lynch, M.E.; Fischbach, C., A Novel 3-D Mineralized Model to Study the Effects of Loading on Bone Metastasis, *Talk presented at Biomedical Engineering Society Annual Meeting*, 2012, Atlanta, GA.

Lee, M.J.; Lynch, M.E.; Fischbach, C., Developing 3-D Culture Models for Investigating the Role of Mechanical Loading on Bone Metastasis, *Talk presented at SILS Undergrad Symposium*, 2012, Ithaca, NY.

Lee, M.J.; Lynch, M.E.; Fischbach, C., A Novel 3-D *In Vitro* Model of the Skeleton for Studying Bone and Metastatic Breast Cancer, *Poster presented at BioExpo*, 2012, Ithaca, NY.

Publications:

Lynch, M. E., Brooks, D., Mohanan, S., Lee, M. J., Polamraju, P., Dent, K., Bonassar, L., van der Meulen, M. C. H. & Fischbach, C. *In Vivo* Tibial Compression Decreases Osteolysis and Tumor Formation in a Human Metastatic Breast Cancer Model. Accepted in *Journal of bone and mineral research : the official journal of the American Society for Bone and Mineral Research*.

References

- 1 Catzavelos, C. *et al.* Decreased levels of the cell-cycle inhibitor p27Kip1 protein: prognostic implications in primary breast cancer. *Nature medicine* **3**, 227-230 (1997).
- 2 Weilbaecher, K. N., Guise, T. A. & McCauley, L. K. Cancer to bone: a fatal attraction. *Nature reviews. Cancer* **11**, 411-425, doi:10.1038/nrc3055 (2011).
- 3 Coleman, R. E. Metastatic bone disease: clinical features, pathophysiology and treatment strategies. *Cancer treatment reviews* **27**, 165-176, doi:10.1053/ctrv.2000.0210 (2001).
- 4 Kozlow, W. & Guise, T. A. Breast cancer metastasis to bone: mechanisms of osteolysis and implications for therapy. *Journal of mammary gland biology and neoplasia* **10**, 169-180, doi:10.1007/s10911-005-5399-8 (2005).
- 5 Mundy, G. R. Metastasis to bone: causes, consequences and therapeutic opportunities. *Nature reviews. Cancer* **2**, 584-593, doi:10.1038/nrc867 (2002).
- 6 Fu, X. *et al.* Migration of bone marrow-derived mesenchymal stem cells induced by tumor necrosis factor-alpha and its possible role in wound healing. *Wound repair and regeneration : official publication of the Wound Healing Society [and] the European Tissue Repair Society* **17**, 185-191, doi:10.1111/j.1524-475X.2009.00454.x (2009).

- 7 Castronovo, V. & Bellahcene, A. Evidence that breast cancer associated microcalcifications are mineralized malignant cells. *International journal of oncology* **12**, 305-308 (1998).
- 8 Tabar, L. *et al.* A novel method for prediction of long-term outcome of women with T1a, T1b, and 10-14 mm invasive breast cancers: a prospective study. *Lancet* **355**, 429-433 (2000).
- 9 Haka, A. S. *et al.* Identifying microcalcifications in benign and malignant breast lesions by probing differences in their chemical composition using Raman spectroscopy. *Cancer research* **62**, 5375-5380 (2002).
- 10 Robling, A. G. & Turner, C. H. Mechanical signaling for bone modeling and remodeling. *Critical reviews in eukaryotic gene expression* **19**, 319-338 (2009).
- 11 Sterling, J. A., Edwards, J. R., Martin, T. J. & Mundy, G. R. Advances in the biology of bone metastasis: how the skeleton affects tumor behavior. *Bone* **48**, 6-15, doi:10.1016/j.bone.2010.07.015 (2011).
- 12 Hillam, R. A. & Skerry, T. M. Inhibition of bone resorption and stimulation of formation by mechanical loading of the modeling rat ulna in vivo. *Journal of bone and mineral research : the official journal of the American Society for Bone and Mineral Research* **10**, 683-689, doi:10.1002/jbmr.5650100503 (1995).
- 13 Chow, J. W., Wilson, A. J., Chambers, T. J. & Fox, S. W. Mechanical loading stimulates bone formation by reactivation of bone lining cells in 13-week-old rats. *Journal of bone and mineral research : the official journal of the American Society for Bone and Mineral Research* **13**, 1760-1767, doi:10.1359/jbmr.1998.13.11.1760 (1998).

- 14 Borer, K. T. Physical activity in the prevention and amelioration of osteoporosis in women : interaction of mechanical, hormonal and dietary factors. *Sports medicine* **35**, 779-830 (2005).
- 15 Milne, H. M., Wallman, K. E., Gordon, S. & Courneya, K. S. Effects of a combined aerobic and resistance exercise program in breast cancer survivors: a randomized controlled trial. *Breast cancer research and treatment* **108**, 279-288, doi:10.1007/s10549-007-9602-z (2008).
- 16 Schwartz, A. L., Winters-Stone, K. & Gallucci, B. Exercise effects on bone mineral density in women with breast cancer receiving adjuvant chemotherapy. *Oncology nursing forum* **34**, 627-633, doi:10.1188/07.ONF.627-633 (2007).
- 17 Lynch, M. E., Brooks, D., Mohanan, S., Lee, M.J., Polamraju, P., Dent, K., Bonassar, L., van der Meulen, M.C.H. & Fischbach, C. *In Vivo* Tibial Compression Decreases Osteolysis and Tumor Formation in a Human Metastatic Breast Cancer Model. Revision in *Journal of bone and mineral research : the official journal of the American Society for Bone and Mineral Research*.
- 18 Fischbach, C. *et al.* Engineering tumors with 3D scaffolds. *Nature methods* **4**, 855-860, doi:10.1038/nmeth1085 (2007).
- 19 Pathi, S. P., Kowalczewski, C., Tadipatri, R. & Fischbach, C. A novel 3-D mineralized tumor model to study breast cancer bone metastasis. *PloS one* **5**, e8849, doi:10.1371/journal.pone.0008849 (2010).
- 20 Pathi, S. P., Lin, D. D., Dorvee, J. R., Estroff, L. A. & Fischbach, C. Hydroxyapatite nanoparticle-containing scaffolds for the study of breast cancer bone metastasis. *Biomaterials* **32**, 5112-5122, doi:10.1016/j.biomaterials.2011.03.055 (2011).

- 21 Minn, A. J. *et al.* Distinct organ-specific metastatic potential of individual breast cancer cells and primary tumors. *The Journal of clinical investigation* **115**, 44-55, doi:10.1172/JCI22320 (2005).
- 22 Bendre, M. S. *et al.* Expression of interleukin 8 and not parathyroid hormone-related protein by human breast cancer cells correlates with bone metastasis in vivo. *Cancer research* **62**, 5571-5579 (2002).
- 23 Mancino, A. T., Klimberg, V. S., Yamamoto, M., Manolagas, S. C. & Abe, E. Breast cancer increases osteoclastogenesis by secreting M-CSF and upregulating RANKL in stromal cells. *The Journal of surgical research* **100**, 18-24, doi:10.1006/jsre.2001.6204 (2001).
- 24 Thomas, R. J. *et al.* Breast cancer cells interact with osteoblasts to support osteoclast formation. *Endocrinology* **140**, 4451-4458 (1999).
- 25 Javed, A. *et al.* Impaired intranuclear trafficking of Runx2 (AML3/CBFA1) transcription factors in breast cancer cells inhibits osteolysis in vivo. *Proceedings of the National Academy of Sciences of the United States of America* **102**, 1454-1459, doi:10.1073/pnas.0409121102 (2005).
- 26 Bu, G. *et al.* Breast cancer-derived Dickkopf1 inhibits osteoblast differentiation and osteoprotegerin expression: implication for breast cancer osteolytic bone metastases. *International journal of cancer. Journal international du cancer* **123**, 1034-1042, doi:10.1002/ijc.23625 (2008).
- 27 Barnes, G. L. *et al.* Fidelity of Runx2 activity in breast cancer cells is required for the generation of metastases-associated osteolytic disease. *Cancer research* **64**, 4506-4513, doi:10.1158/0008-5472.CAN-03-3851 (2004).

- 28 Mendoza-Villanueva, D., Zeef, L. & Shore, P. Metastatic breast cancer cells inhibit osteoblast differentiation through the Runx2/CBFBeta-dependent expression of the Wnt antagonist, sclerostin. *Breast cancer research : BCR* **13**, R106, doi:10.1186/bcr3048 (2011).
- 29 Zhang, S. *et al.* Dose-dependent effects of Runx2 on bone development. *Journal of bone and mineral research : the official journal of the American Society for Bone and Mineral Research* **24**, 1889-1904, doi:10.1359/jbmr.090502 (2009).
- 30 Ducy, P., Zhang, R., Geoffroy, V., Ridall, A. L. & Karsenty, G. Osf2/Cbfa1: a transcriptional activator of osteoblast differentiation. *Cell* **89**, 747-754 (1997).
- 31 Karsenty, G., Kronenberg, H. M. & Settembre, C. Genetic control of bone formation. *Annual review of cell and developmental biology* **25**, 629-648, doi:10.1146/annurev.cellbio.042308.113308 (2009).
- 32 Di Benedetto, A. *et al.* N-cadherin and cadherin 11 modulate postnatal bone growth and osteoblast differentiation by distinct mechanisms. *Journal of cell science* **123**, 2640-2648, doi:10.1242/jcs.067777 (2010).
- 33 Rhodes, L. V. *et al.* Effects of human mesenchymal stem cells on ER-positive human breast carcinoma cells mediated through ER-SDF-1/CXCR4 crosstalk. *Molecular cancer* **9**, 295, doi:10.1186/1476-4598-9-295 (2010).
- 34 Finger, A. R., Sargent, C. Y., Dulaney, K. O., Bernacki, S. H. & Lobo, E. G. Differential effects on messenger ribonucleic acid expression by bone marrow-derived human mesenchymal stem cells seeded in agarose constructs due to ramped and steady applications of cyclic hydrostatic pressure. *Tissue engineering* **13**, 1151-1158, doi:10.1089/ten.2006.0290 (2007).

- 35 Tanaka, S. M., Sun, H. B. & Yokota, H. Bone formation induced by a novel form of mechanical loading on joint tissue. *Uchu Seibutsu Kagaku* **18**, 41-44 (2004).
- 36 Ballyns, J. J. & Bonassar, L. J. Dynamic compressive loading of image-guided tissue engineered meniscal constructs. *Journal of biomechanics* **44**, 509-516, doi:10.1016/j.jbiomech.2010.09.017 (2011).
- 37 Sittichokechaiwut, A., Scutt, A. M., Ryan, A. J., Bonewald, L. F. & Reilly, G. C. Use of rapidly mineralising osteoblasts and short periods of mechanical loading to accelerate matrix maturation in 3D scaffolds. *Bone* **44**, 822-829, doi:10.1016/j.bone.2008.12.027 (2009).
- 38 Schmittgen, T. D. & Livak, K. J. Analyzing real-time PCR data by the comparative C(T) method. *Nature protocols* **3**, 1101-1108 (2008).
- 39 Chomczynski, P. & Sacchi, N. Single-step method of RNA isolation by acid guanidinium thiocyanate-phenol-chloroform extraction. *Analytical biochemistry* **162**, 156-159, doi:10.1006/abio.1987.9999 (1987).
- 40 Kretlow, J. D. *et al.* Donor age and cell passage affects differentiation potential of murine bone marrow-derived stem cells. *BMC cell biology* **9**, 60, doi:10.1186/1471-2121-9-60 (2008).
- 41 Li, O. *et al.* Human embryonic stem cell-derived mesenchymal stroma cells (hES-MSCs) engraft in vivo and support hematopoiesis without suppressing immune function: implications for off-the shelf ES-MSC therapies. *PloS one* **8**, e55319, doi:10.1371/journal.pone.0055319 (2013).

- 42 Bendre, M. S. *et al.* Interleukin-8 stimulation of osteoclastogenesis and bone resorption is a mechanism for the increased osteolysis of metastatic bone disease. *Bone* **33**, 28-37 (2003).
- 43 de Peppo, G. M. *et al.* Human embryonic mesodermal progenitors highly resemble human mesenchymal stem cells and display high potential for tissue engineering applications. *Tissue engineering. Part A* **16**, 2161-2182, doi:10.1089/ten.TEA.2009.0629 (2010).
- 44 Pratap, J. *et al.* Runx2 transcriptional activation of Indian Hedgehog and a downstream bone metastatic pathway in breast cancer cells. *Cancer research* **68**, 7795-7802, doi:10.1158/0008-5472.CAN-08-1078 (2008).
- 45 Schwartz, A. L., Mori, M., Gao, R., Nail, L. M. & King, M. E. Exercise reduces daily fatigue in women with breast cancer receiving chemotherapy. *Medicine and science in sports and exercise* **33**, 718-723 (2001).
- 46 Winters-Stone, K. M. *et al.* The effect of resistance training on muscle strength and physical function in older, postmenopausal breast cancer survivors: a randomized controlled trial. *Journal of cancer survivorship : research and practice* **6**, 189-199, doi:10.1007/s11764-011-0210-x (2012).
- 47 Vainionpaa, A., Korpelainen, R., Leppaluoto, J. & Jamsa, T. Effects of high-impact exercise on bone mineral density: a randomized controlled trial in premenopausal women. *Osteoporosis international : a journal established as result of cooperation between the European Foundation for Osteoporosis and the National Osteoporosis Foundation of the USA* **16**, 191-197, doi:10.1007/s00198-004-1659-5 (2005).

- 48 Stengel, S. V. *et al.* Power training is more effective than strength training for maintaining bone mineral density in postmenopausal women. *Journal of applied physiology* **99**, 181-188, doi:10.1152/jappphysiol.01260.2004 (2005).
- 49 Nguyen, D. X., Bos, P. D. & Massague, J. Metastasis: from dissemination to organ-specific colonization. *Nature reviews. Cancer* **9**, 274-284, doi:10.1038/nrc2622 (2009).
- 50 Yae, T. *et al.* Alternative splicing of CD44 mRNA by ESRP1 enhances lung colonization of metastatic cancer cell. *Nature communications* **3**, 883, doi:10.1038/ncomms1892 (2012).
- 51 Blanco, M. A. & Kang, Y. Signaling pathways in breast cancer metastasis - novel insights from functional genomics. *Breast cancer research : BCR* **13**, 206, doi:10.1186/bcr2831 (2011).

Supplemental Table and Figure

Table S1: Primer sequences used for quantitative RT-PCR (qPCR). Gene expressions commonly associated with bone metastasis (OPN, MMP1, and CXCR4) and osteolysis (IL-8, RANK, DKK, Runx2) were analyzed using qPCR and the comparative ΔC_T method 24 hours after the last loading session.

Gene	Name	Primer Sequence	
<i>Runx2</i>	runt related transcription factor 2	CCAACCCACGAATGCACTATC	Forward
		TAGTGAGTGGTGGCGGACATA	Reverse
<i>RANK</i>	Receptor Activator of Nuclear Factor κ B	CACCAAATGAACCCCATGTTTAC	Forward
		GGACTCCTTATCTCCACTTAGGC	Reverse
<i>DKK1</i>	dickkopf 1 homolog	ATAGCACCTTGGATGGGTATTCC	Forward
		CTGATGACCGGAGACAAACAG	Reverse
<i>OPN</i>	Osteopontin	TGAGAGCAATGAGCATTCGGATG	Forward
		CAGGGAGTTTCCATGAAGCCAC	Reverse
<i>IL-8</i>	interleukin 8	AGGTGCAGTTTTGCCAAGGA	Forward
		TTTCTGTGTTGGCGCAGTGT	Reverse
<i>MMP1</i>	matrix metalloproteinase 1	AAATGCAGGAATTCTTTGGG	Forward
		ATGGTCCACATCTGCTCTTG	Reverse
<i>CXCR4</i>	chemokine (C-X-C motif) receptor 4	GCCTTATCCTGCCTGGTATTGTC	Forward
		GCGAAGAAAGCCAGGATGAGGAT	Reverse
<i>Actb</i>	beta-actin	AATGTGGCCGAGGACTTTGATTGC	Forward
		AGGATGGCAAGGGACTTCCTGTAA	Reverse

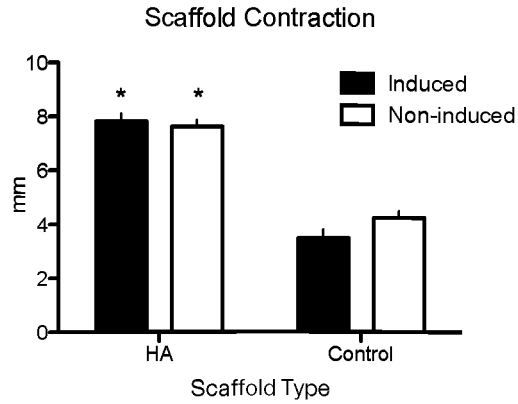
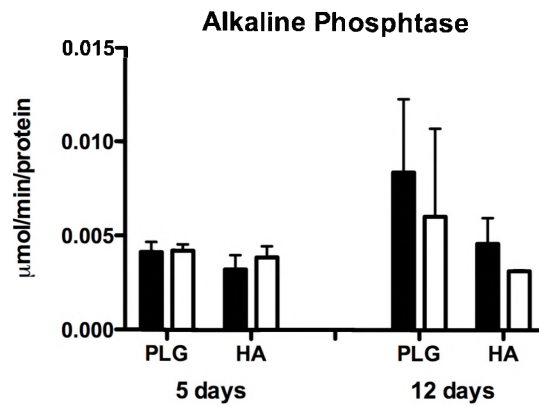


Fig. S1: Scaffold contraction after 60 days of culture with BM-MSCs. Scaffold diameter decreased substantially for control scaffolds (-50%, pooled average), whereas HA scaffolds maintained their shape after 60 days of culture. * the effect of HA scaffolds vs. PLG (comparisons made within and induced and non-induced condition separately).

A.



B.

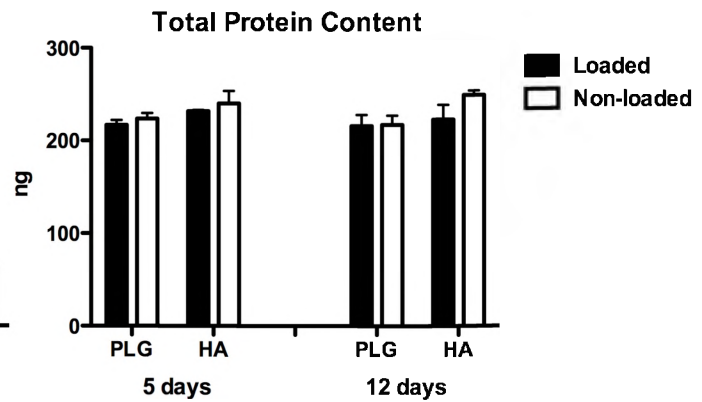


Fig. S2: Normalized ALP activity and total protein content assay of lysates prepared from BM-MSCs after hydrostatic loading. (A) ALP expression did not increase after 5 days of loading and did not show sustained effects of loading after a week (12 days). (B) Loading did not have any effect on total protein content of BM-MSCs.